INTERNATIONAL JOURNAL FOR NUMERICAL METHODS IN FLUIDS, VOL. 16, 915–929 (1993)

FLOW REGIMES AND FREQUENCY SELECTION OF A CYLINDER OSCILLATING IN AN UPSTREAM CYLINDER WAKE

J. SUN

LRC, Université de Provence, 13397 Marseille Cedex 13, France

AND

J. LI AND B. ROUX

Institut de Mécanique des Fluides, 1, Rue Honnorat, 13003 Marseille, France

SUMMARY

This paper describes flow around a pair of cylinders in tandem arrangement with a downstream cylinder being fixed or forced to oscillate transversely. A sinusoidal parietal velocity is applied to simulate cylinder oscillation. Time-dependent Navier–Stokes equations are solved using finite element method. It is shown that there exist two distinct flow regimes: 'vortex suppression regime' and 'vortex formation regime'. Averaged vortex lengths between the two cylinders, pressure variations at back and front stagnant points as well as circumferential pressure profiles of the downstream cylinder are found completely different in the two regimes and, thus, can be used to identify the flow regimes. It is shown that frequency selection in the wake of the oscillating cylinder is a result of non-linear interaction among vortex wakes upstream and downstream of the second cylinder and its forced oscillation. Increasing cylinder spacing results in a stronger oscillatory incident flow upstream of the second cylinder and, thus, a smaller synchronization zone.

KEY WORDS Cylinder oscillation Frequency selection Lock-in Vortex formation regime Vortex suppression regime Wake flow

1. INTRODUCTION

Flow–structure interaction commonly occurs in arrays of cylinders subjected to crossflow. Investigation of such flow interference is important in the area of flow-induced vibration. It is well known that wake-related Strouhal-type periodicities can sometimes lead to resonances of the structure. Oscillation of the cylinder can also cause the vortex shedding pattern to change and the vortex shedding frequency to shift. Information about the response states that develop in the wake of an oscillating cylinder is essential for active control of the vortex wake. In the past decades, advances have been made in the understanding of the fundamental phenomena of cylinder–vortex-wake interactions. These advances have resulted in a number of new theories explaining the discontinuous Reynolds-number–Strouhal-number relation, the transition to turbulence in open flows, and so on.[1–3] However, in most of these studies, emphasis has been given to the role played by the oscillation of the cylinder in which the incident flow is assumed to be uniform. More complex cases such as the wake–cylinder–wake system are more frequently encountered in practical occasions. An oscillating cylinder placed in the wake of upstream

0271–2091/93/100915–15$12.50

Received January 1992
Revised December 1992

cylinders is a simple example of such an interaction system. The investigation of frequency selection in a wake–cylinder-oscillation–wake system can offer significant insight into the understanding of the interactions of the laminar wakes.

For a cylinder oscillating in uniform flow, when the external forcing frequency is approached to the natural vortex shedding frequency, the latter may be drifted towards the forcing frequency and be locked on to it. This phenomena is denoted as 'lock-in' or 'synchronization'. On the contrary, if the forcing frequency is sufficiently far from the natural shedding frequency, both forcing and shedding frequencies will be detected in the wake. In some cases, vortex shedding frequency may differ from natural shedding frequency,[4,5] but it is still distinguishable from the forcing frequency. This response state is denoted as 'non-lock-in' state.[6,7] For a cylinder oscillating in the wake of another cylinder, the same concept can be applied. In fact, both response states can be obtained, depending upon the flow conditions.[5,8]

In the present work, the simplest system of wake–cylinder-oscillation–wake is considered, which contains a pair of cylinders in tandem arrangement with a downstream cylinder oscillating transversely. Although geometrically simple, it pertains the basic characteristics of a tube–array system. Flow characteristics and flow regimes are studied. The influence of oscillatory wake flow upstream of an oscillating cylinder on its lock-in range is assessed by changing the distance between the two cylinders. Finally, the numerical results obtained are compared with experimental data of Tanida *et al.*[2]

2. MATHEMATICAL FORMULATION AND SOLUTION PROCEDURE

We consider two cylinders placed in tandem. Computational domain is depicted in Figure 1. We assume that flow is isothermal, incompressible and Newtonian. The governing equation consists of the equation of continuity and the momentum equation written in their dimensionless form as follows:

$$\nabla \cdot \mathbf{u} = 0, \tag{1}$$

$$\frac{\partial \mathbf{u}}{\partial t} + \mathbf{u} \cdot \nabla \mathbf{u} = -\nabla p + \frac{1}{Re} \nabla^2 \mathbf{u}, \tag{2}$$

where $\mathbf{u} = (u, v)$ is the velocity vector, $Re = U_\infty D/\nu$ denotes the Reynolds number, D the diameter

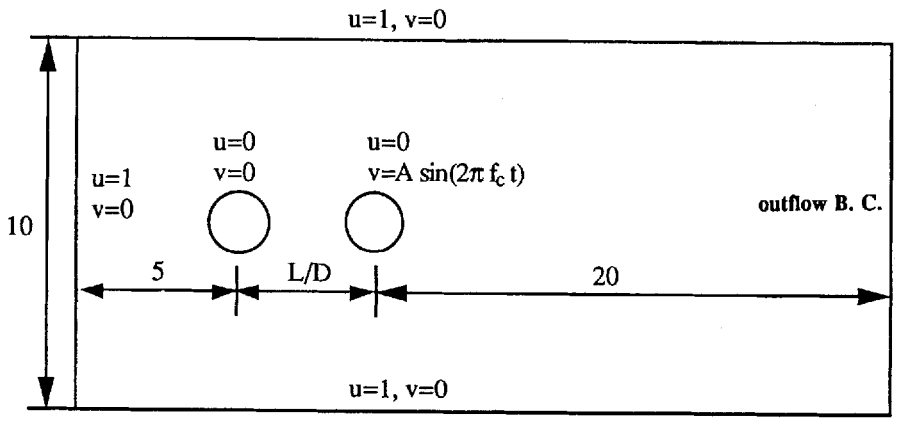

Figure 1. Computational domain

of the cylinder, U_∞ the free-stream velocity and ν the kinematic viscosity of the fluid. All lengths are scaled by D, and all velocities by U_∞.

No-slip conditions are imposed on the upstream cylinder while the downstream cylinder has a sinusoidal velocity if there is an external forcing:

upstream cylinder:

$$u=0, \qquad v=0, \tag{3}$$

downstream cylinder:

$$u=0, \qquad v=\begin{cases} A\sin(2\pi f_c t) & \text{with forcing,} \\ 0 & \text{without forcing,} \end{cases} \tag{4}$$

where f_c is the forcing frequency and A the velocity amplitude of cylinder oscillation. This forcing corresponds to a parietal velocity, i.e. aspiration and transpiration through the cylinder wall. For sufficiently large computational domain, as the one used in the present work (Figure 1), flow perturbation due to the presence of the cylinders at the inlet, upper and lower boundaries is negligible. Therefore, we suppose that flow velocity reaches the free-stream value at these boundaries: $u=1, v=0$. Free outflow conditions (natural boundary conditions) are imposed at the outlet boundary:[9]

$$-p+\frac{2}{Re}\frac{\partial u}{\partial x}=0, \tag{5}$$

$$\frac{1}{Re}\left(\frac{\partial u}{\partial y}+\frac{\partial v}{\partial x}\right)=0. \tag{6}$$

It is noted that the forcing mechanism used in the present work is not strictly equivalent to a real oscillating cylinder. Since the motion of downstream cylinder has two effects: the velocity effect, and another effect caused by the displacement of the cylinder which changes the system geometry. However, for small-amplitude oscillations (as in the present study where $A<0{\cdot}2$), the displacement of the cylinder is very small and, thus, has minor effects on basic characteristics of the system. In this case, the parietal velocity forcing is a good approximation of the problem. This assumption can be verified from the results in Section 3. Further verification was made by applying such forcing onto a single cylinder to simulate its oscillation. The results thus obtained are compared with the results found in the literature where a transformation of co-ordinates was performed to simulate cylinder motion;[10] similar results are found. One of the major advantages of the present forcing is that it is very simple and easy to be dealt with numerically. Moreover, this forcing mechanism can be easily applied to multiple-cylinder systems in which some of the cylinders may oscillate (in phase or out of phase) while others remain at rest. The co-ordinate transformation method in such a case is inapplicable because the system is far too complicated. Nevertheless, it should be remarked that parietal velocity forcing is valid only for small-amplitude oscillations; the displacement effect should be taken into account when the amplitude of cylinder oscillation is large.

Time-dependent Navier–Stokes equations are solved in terms of its primitive variables using finite element method. Galerkin finite element approach is applied for the discretization of the governing equation. Nine-node quadratic and quadrilateral elements are used for the velocity while bilinear interpolation function for the pressure. Temporal discretization is performed using Crank–Nicolson scheme. It is non-dissipative, second-order-accurate and completely stable. The discretization in time and space results in the following non-linear system:

$$[K(U)]\{U\}=\{F\}, \tag{7}$$

with $U=\{U_i\}$ and $U_i=(u_i, v_i, p_i)$ at node i, $K(U)$ is a non-linear matrix. Equation (7) is solved using Newton–Ralphson method. Finer mesh is generated in the vicinity of the cylinders where boundary layers are formed. Cylinder spacings are varied between $L/D=2{\cdot}5$ and $L/D=8{\cdot}0$ to study flow interferences and vortex shedding characteristics. Solutions with fully developed vortex streets are obtained first, which serve as initial conditions for subsequent computations with forced oscillation. For each spacing, forcing frequency is swept around f_{s0} in order to determine the synchronization range (f_{s0} denotes vortex shedding frequency without forced oscillation).

The forces exerted on the cylinders are calculated at each time step. The drag and the lift coefficients are determined by the following formulae:

$$C_D=2\oint_{\text{cylinder}}\left\{-p\,dx+\frac{1}{Re}\left[2\frac{\partial u}{\partial x}dx+\left(\frac{\partial u}{\partial y}+\frac{\partial v}{\partial x}\right)dy\right]\right\}, \tag{8}$$

$$C_L=2\oint_{\text{cylinder}}\left\{-p\,dy+\frac{1}{Re}\left[\left(\frac{\partial u}{\partial y}+\frac{\partial v}{\partial x}\right)dx+2\frac{\partial v}{\partial y}dy\right]\right\}. \tag{9}$$

The consistency in mesh refinement is also tested, showing that the mesh used in the present work (2697 nodal points and 640 elements) is sufficient for global error control of flow quantities. All computations are carried out on a single processor of an Intel iPSC/860 computer.

3. FLOW REGIMES AND FLOW CHARACTERISTICS

We first discuss different flow regimes for two tandem cylinders placed in crossflow. Both experimental and numerical results have shown the existence of a critical cylinder spacing $(L/D)_{cr}$ characterizing two different flow regimes, referred to as 'vortex suppression (VS) regime' and 'vortex formation (VF) regime'.[5,8,9,11,12] Vortex suppression regime occurs when the spacing between the two cylinders is inferior to the critical spacing. In this regime, the shear layers separating from the upstream cylinder reattach to the downstream cylinder so that vortices do not have sufficient room to grow, to develop and to shed. Since the downstream cylinder is in the attached vortex region of the upstream cylinder, its equivalent oncoming 'free-stream' velocity is quite weak. This leads to an even weaker wake behind it. Although in almost all cases there is no evident oscillation in the near wake of the downstream cylinder, visible or strong oscillations are observed in the far wake from the numerical simulation (Figure 2(a)).

When the spacing between the two cylinders is greater than its critical value, a vortex formation regime appears and vortex streets form behind both cylinders. The occurrence of vortex shedding between the two cylinders creates oscillatory oncoming flow upstream of the second cylinder, and this leads to a stronger oscillatory flow behind the downstream cylinder. In Figure 2, we show the velocity fields in two flow regimes for one complete shedding cycle ($Re=100$, at $L/D=2{\cdot}5$ (the VS regime) and $L/D=4{\cdot}5$ (the VF regime)).

The two flow regimes can also be distinguished by examining the time-averaged vortex length l_v between the two cylinders. This length l_v is defined as the distance from the back stagnant point of the upstream cylinder to the point on the centreline at which the time-averaged velocities $\bar{u}=\bar{v}=0$. This point is denoted as 'time-averaged stagnant point', shown in Figure 3. Figure 4 shows the vortex lengths l_v as a function of cylinder spacing L/D. In the VS regime, since the vortices behind the first cylinder have no room to develop, no detachment occurs. And the vortex length is simply equal to the distance between the two cylinders (from the back stagnation point of the first cylinder to the front stagnation point of the second cylinder). Thus, l_v is found to

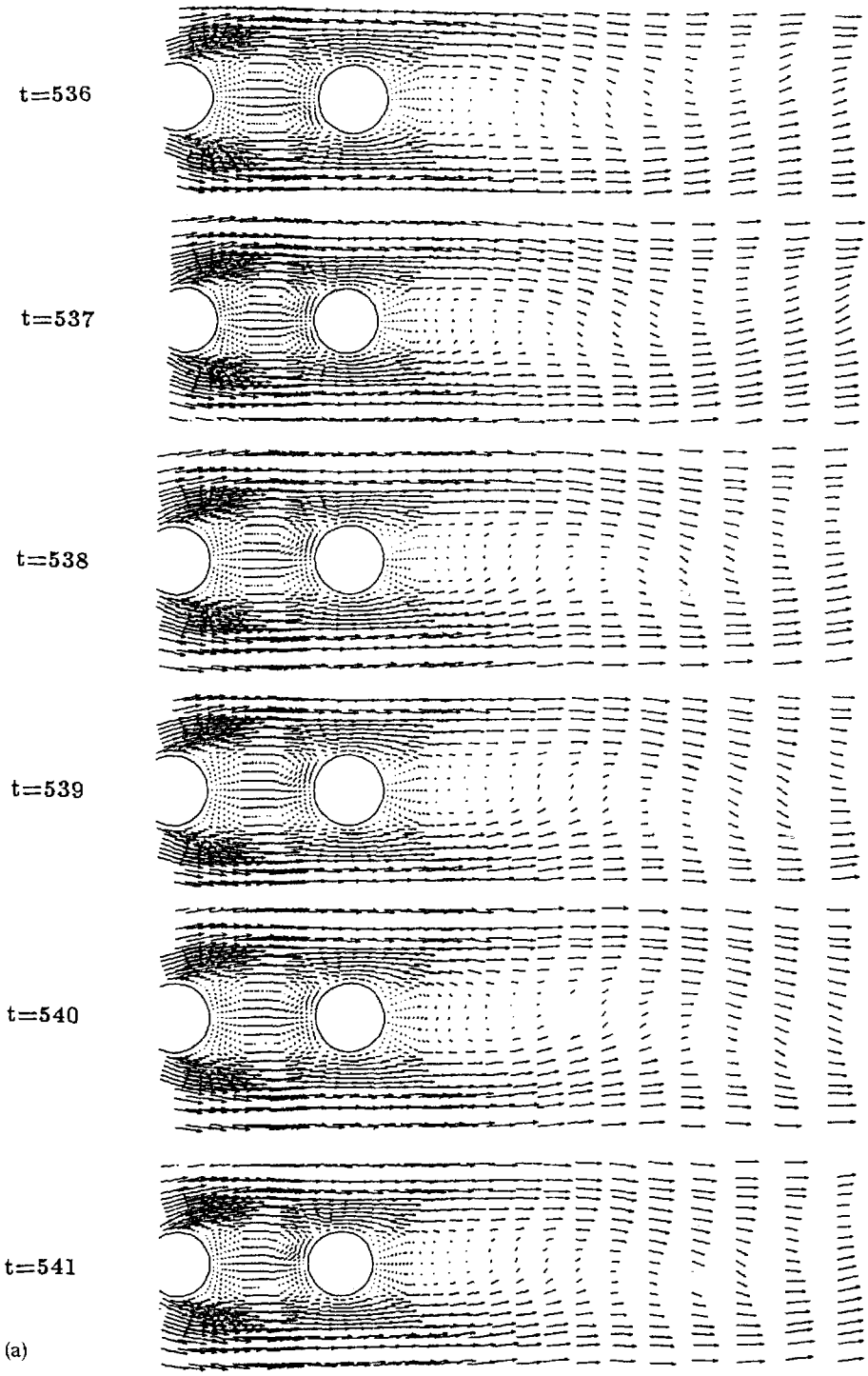

Figure 2. Flow fields for one complete vortex shedding cycle ($Re = 100$): (a) $L/D = 2{\cdot}5$, VS regime; (b) $L/D = 4{\cdot}5$, VF regime

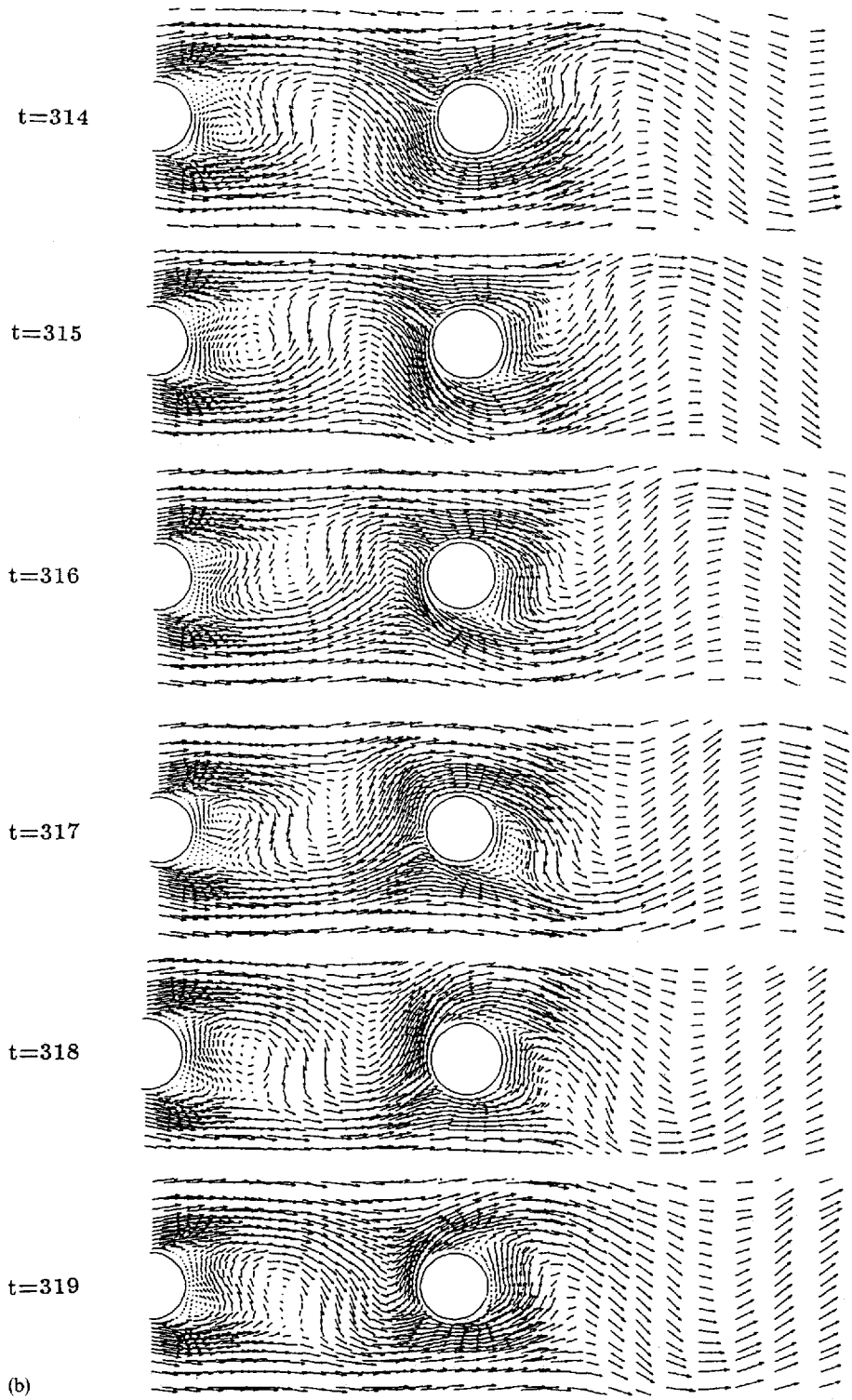

(b)

Figure 2. (Continued)

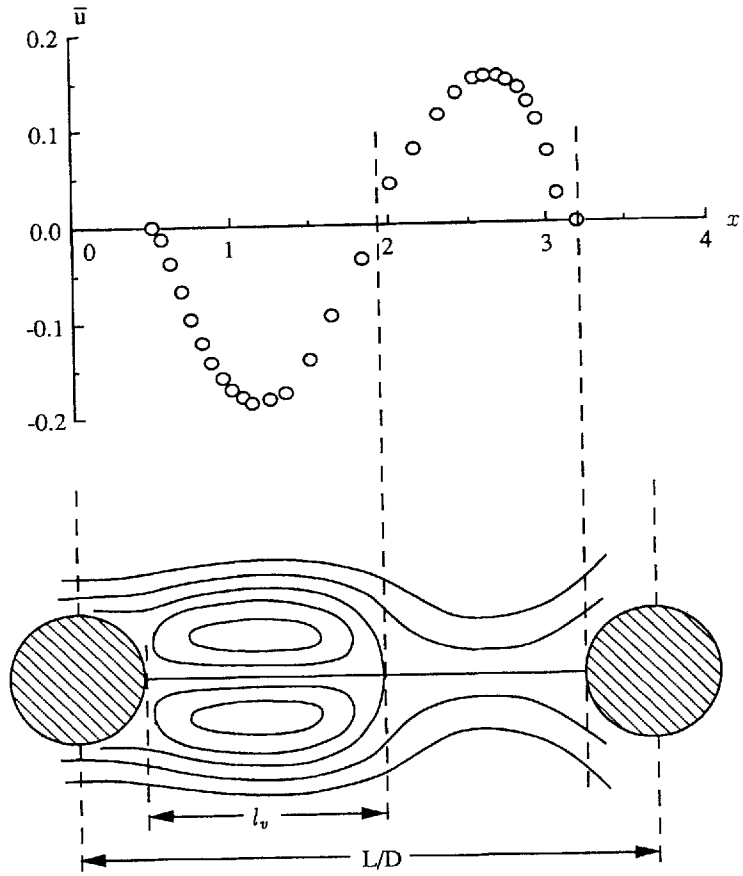

Figure 3. Averaged longitudinal velocity $\bar{u}$ variation in centreline ($y=0$) for $L/D=3{\cdot}7$ and $Re=100$, and the definition of vortex length l_v

increase linearly with L/D. In the VS regime, when L/D is increased, the vortices have more room to grow and stretch, they do not break down and shed off until they reach the maximum stable length. So, the spacing at which the maximum stable vortex length is reached is the critical spacing separating the two flow regimes. Once the vortices begin to shed off, the time-averaged stagnation point is different from the front stagnation point of the downstream cylinder, and the averaged vortex length becomes shorter. The downstream cylinder acts as an obstacle in the vortex street of the upstream cylinder. In the VF regime, with increasing L/D, the vortex street between the two cylinders develops more freely and is more strong, so that vortex length decreases and approaches asymptotically the value of freely shedded vortices at large spacing.

The circumferential pressure distributions of the two cylinders are also different in the two regimes.[5,9,11,12] In the VF regime, the shapes of circumferential pressure profile on upstream and downstream cylinders are similar, with one maximum corresponding to the front stagnant pressure. This means that the flow pattern near the two cylinders are analogous. However, in the VS regime, while the pressure distribution of the upstream cylinder still remains similar, that of the downstream cylinder shows two maxima corresponding to the two reattachment points. The disappearance of the maximum front stagnant point of the downstream cylinder indicates a change in flow pattern. From circumferential pressure distribution of the downstream cylinder,

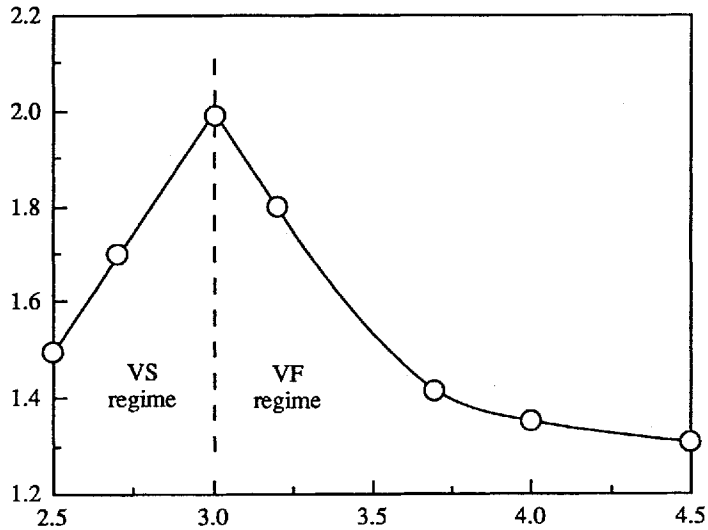

Figure 4. Variation of averaged vortex length l_v versus the cylinder spacing L/D ($Re=100$)

one can easily identify the two flow regimes. In Figure 5, we plot pressure variations at front and back stagnant points of both cylinders as a function of cylinder spacing at $Re=100$. As one may expect, the pressures on the upstream cylinder do not change much with respect to L/D, whereas the pressures on the downstream cylinder have completely different variations. At small spacings,

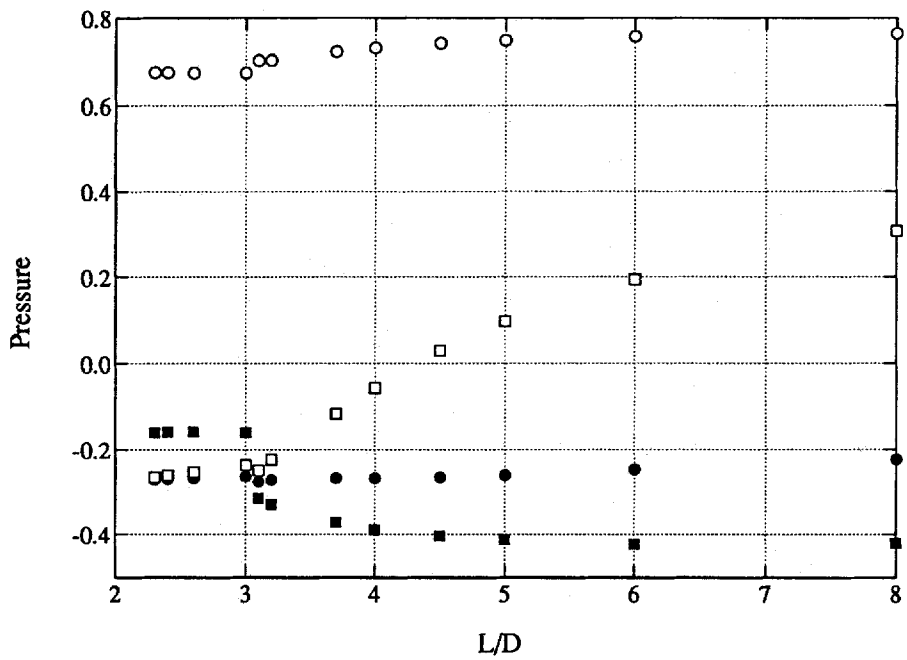

Figure 5. Front and back stagnant pressures of both cylinders versus the cylinder spacing L/D ($Re=100$): (○) front stagnant pressure of upstream cylinder; (●) back stagnant pressure of upstream cylinder; (□) front stagnant pressure of downstream cylinder; (■) back stagnant pressure of downstream cylinder

the pressure of the downstream cylinder is higher at the back stagnant point than at the front stagnant point, so that its drag coefficient may be negative, as is observed in some experiments.[12]

The change of flow regime also causes discontinuous jumps in drag and lift coefficients at critical spacing. The drag coefficient of the upstream cylinder is less influenced by the change of flow regime, since its oncoming flow remains uniform (Figure 6). The lift coefficients of both cylinders jump from almost zero to positive values (Figure 7). The upstream cylinder has a larger

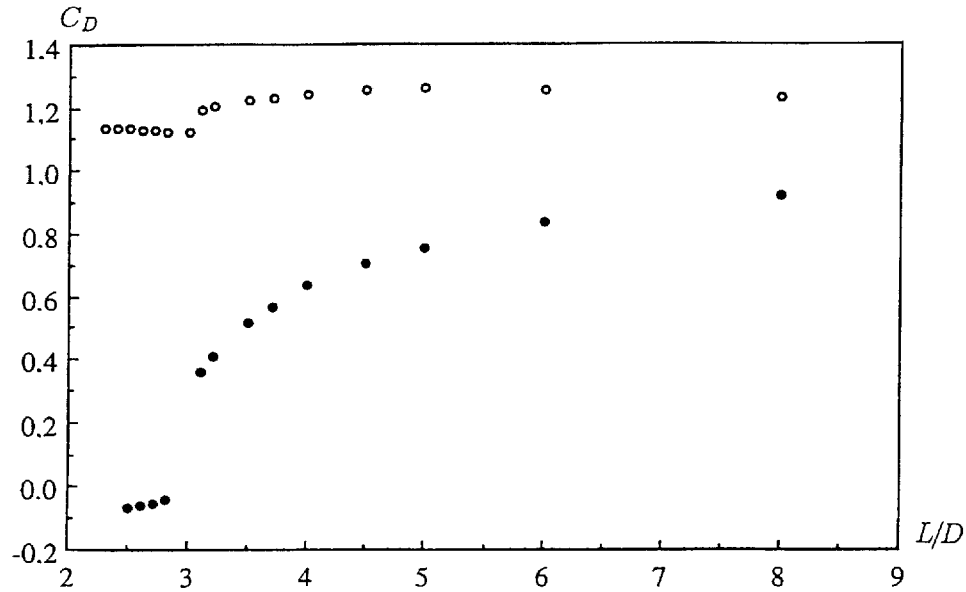

Figure 6. Drag coefficients versus cylinder spacing L/D at $Re = 100$: (○) upstream cylinder; (●) downstream cylinder

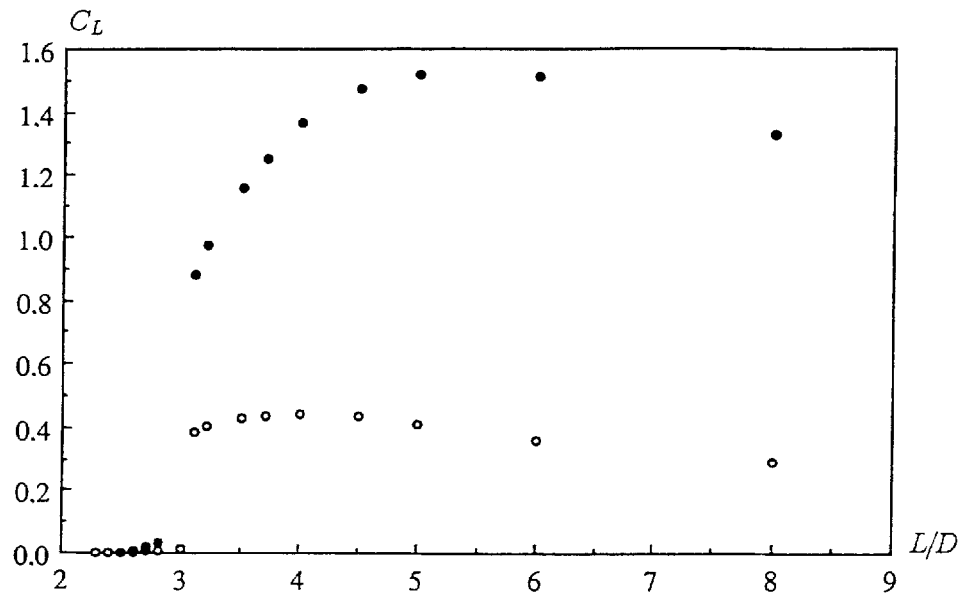

Figure 7. Lift coefficients versus cylinder spacing L/D at $Re = 100$: (○) upstream cylinder; (●) downstream cylinder

drag but a smaller lift coefficient, indicating that oscillation is stronger in the downstream cylinder wake; therefore, the jumps are steeper for the downstream cylinder.

4. WAKE–CYLINDER-OSCILLATION–WAKE INTERACTION

In Section 3, we discussed the flow regimes and their influences on flow characteristics. To understand how flow regimes affect frequency selection in the presence of forced oscillation, we consider the case in which the downstream cylinder is forced to oscillate transversely in the wake of the upstream cylinder. In order to compare with the available experimental data, we chose $Re=80$ and $A/2\pi f_c=0{\cdot}14$. Critical spacing for $Re=80$ is determined to be 3·7 from our numerical data.[5] The critical spacing is found to decrease when the Reynolds number is increased. Since the cylinder oscillates in the wake of another cylinder, frequency selection of its vortex wake depends not only on its downstream wake and its oscillation but also on its oncoming wake flow. Changing the cylinder spacing results in different flow regimes, thus leading to different response states. These response states can be determined from time histories of velocity components, from drag and lift coefficients and their corresponding power spectral density plots. It should also be noted that after we apply the forced oscillation onto the cylinder, the system undergoes a transition to the establishment of the final response states (lock-in or non-lock-in state). We studied only these final states. The moment of applying the initial forcing (i.e. the initial phase angle between the shedding frequency and the forcing frequency) seems not to affect the numerical results obtained.

In Figures 8 and 9, time histories of drag and lift coefficients of the downstream cylinder at different driving frequencies are plotted, respectively. Cylinder spacing is $L/D=4$ and natural vortex shedding frequency f_{s0} is 0·144. Forcing frequency f_c is varied between $1{\cdot}02f_{s0}$ and $1{\cdot}20f_{s0}$. When f_c gradually approaches the natural shedding frequency f_{s0}, the slowly varying period becomes longer and longer until it disappears completely (corresponding to an infinite slowly varying cycle). In fact, this slow-varying cycle corresponds to the harmonic of the system with a frequency equal to $|f_c-f_s|$. Drag and lift coefficients change from composite wave forms (quasiperiodic non-lock-in behaviour) to sinusoidal wave forms (periodic lock-in behaviour). Their corresponding power spectral density plots are shown in Figure 10 (the slow-varying frequencies are not shown because they are outside the frequency range of the plots). For quasiperiodic responses, both forcing frequency f_c and shedding frequency f_s are detected in the spectra. Note that f_s may be slightly different from f_{s0} due to forced oscillation.[4, 5] For periodic response, vortex shedding frequency synchronizes with forcing frequency and the vortex wake is well organized.

By changing the paramters, one can determine the lock-in range as functions of both forcing frequency and cylinder spacing. In Figure 11, we plot the lock-in zone as a function of these parameters. Experimental data of Tanida *et al.*[8] are also plotted in the diagram. In the VS regime, a large lock-in range is obtained because of the weak oncoming flow upstream of the oscillating cylinder. In the VF regime, it is the opposite. The reason is that strong oscillatory oncoming flow reinforces vortex shedding from the downstream cylinder at its natural shedding frequency and, thus, makes it very difficult for the vortex shedding frequency to be locked by the driving frequency. At sufficiently large L/D, no lock-in is observed in our simulation. Experimental data show a similar variation. The discrepancy in lock-in range between $L/D=3{\cdot}5$ and 5·0 comes from the difference in critical cylinder spacing $(L/D)_{cr}$ between the experiments and the numerical simulations. Tanida *et al.*[8] found it 5·0 instead of 3·7 in their experiments, which may possibly be attributed to the 3D effects in the experiments.[3] Despite such a discrepancy, qualitative good agreement between experiments and numerical simulations is still observed. This has shown that

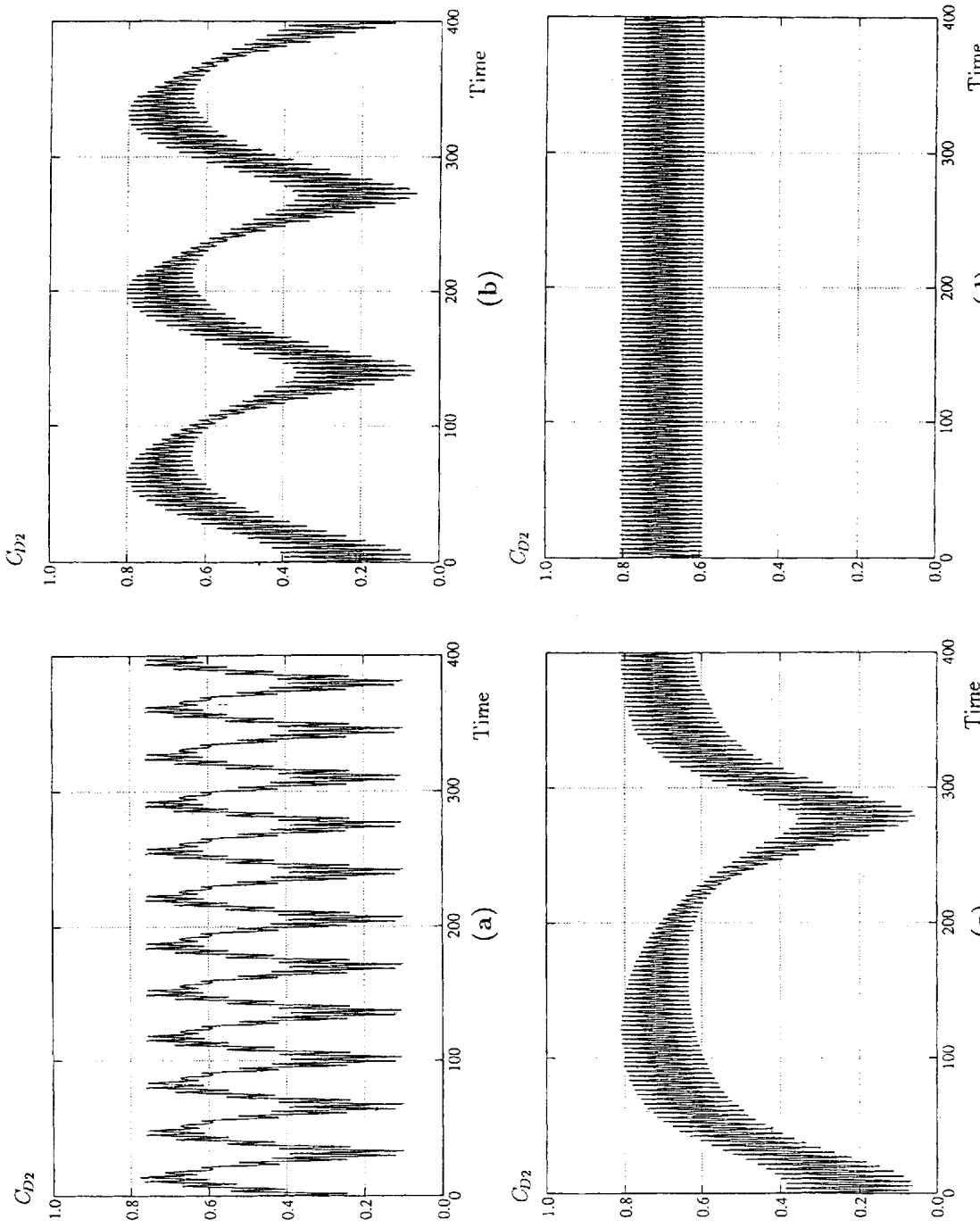

Figure 8. Time histories of the downstream cylinder drag coefficient at different forcing frequencies ($L/D=4{\cdot}0$ and $Re=80$): (a) $f_e=1{\cdot}20f_{s0}$; (b) $f_e=1{\cdot}05f_{s0}$; (c) $f_e=1{\cdot}03f_{s0}$; (d) $f_e=1{\cdot}02f_{s0}$

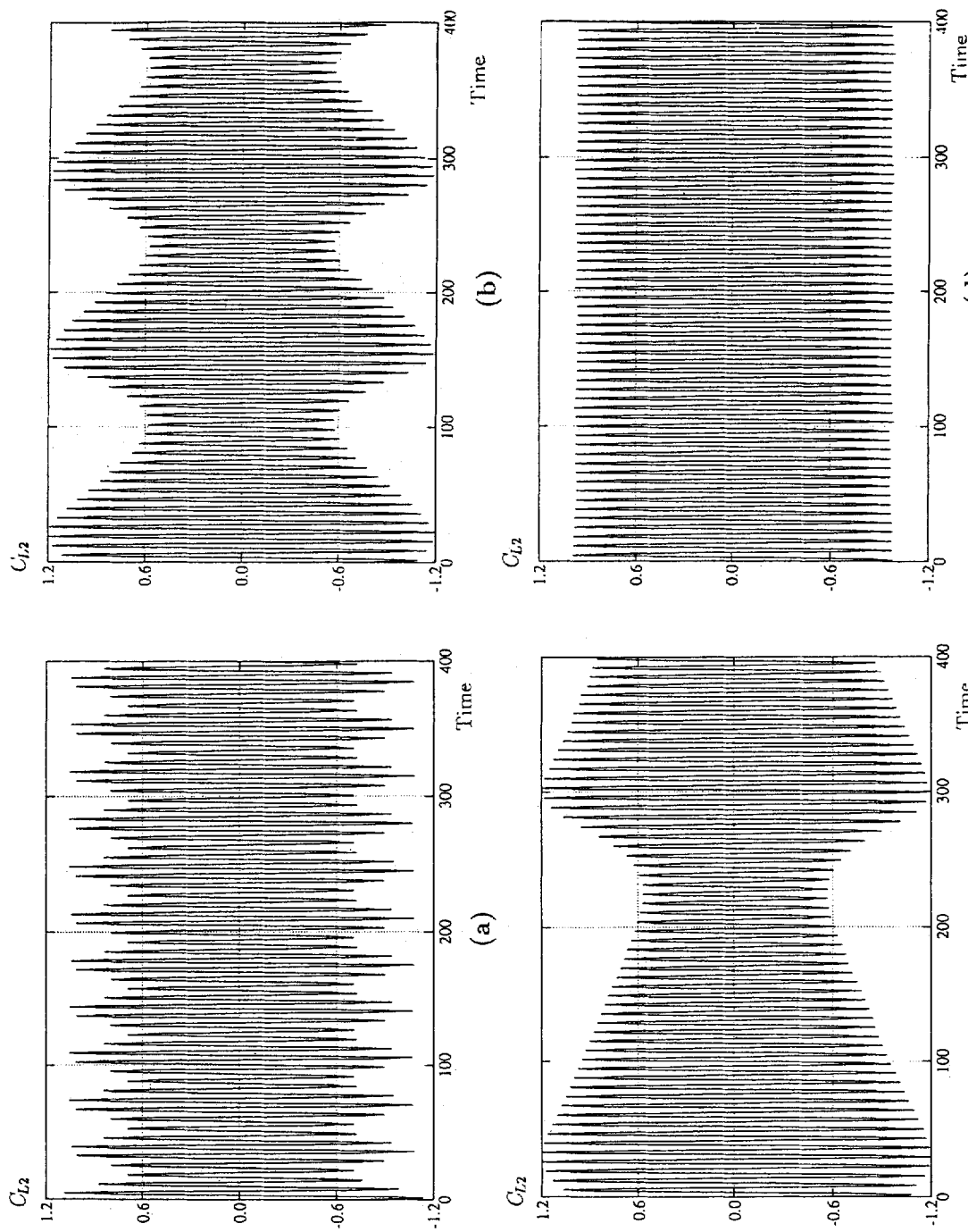

Figure 9. Time histories of the downstream cylinder lift coefficient at different forcing frequencies ($L/D = 4{\cdot}0$ and $Re = 80$): (a) $f_e = 1{\cdot}20 f_{s0}$; (b) $f_e = 1{\cdot}05 f_{s0}$; (c) $f_e = 1{\cdot}03 f_{s0}$; (d) $f_e = 1{\cdot}02 f_{s0}$

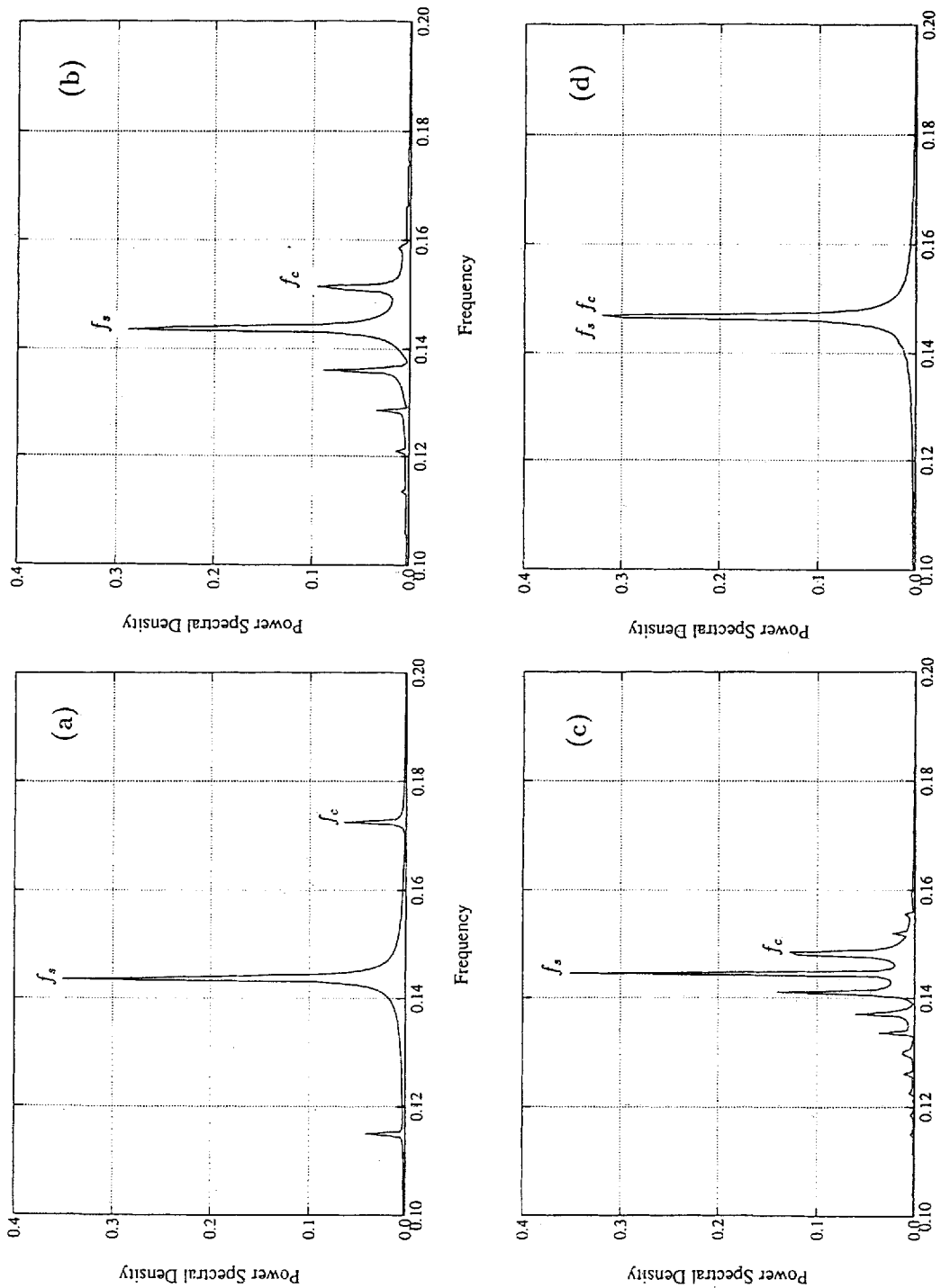

Figure 10. Power spectral densities at different forcing frequencies ($L/D = 4{\cdot}0$ and $Re = 80$): (a) $f_c = 1{\cdot}20 f_{s0}$; (b) $f_c = 1{\cdot}05 f_{s0}$; (c) $f_c = 1{\cdot}03 f_{s0}$; (d) $f_c = 1{\cdot}02 f_{s0}$

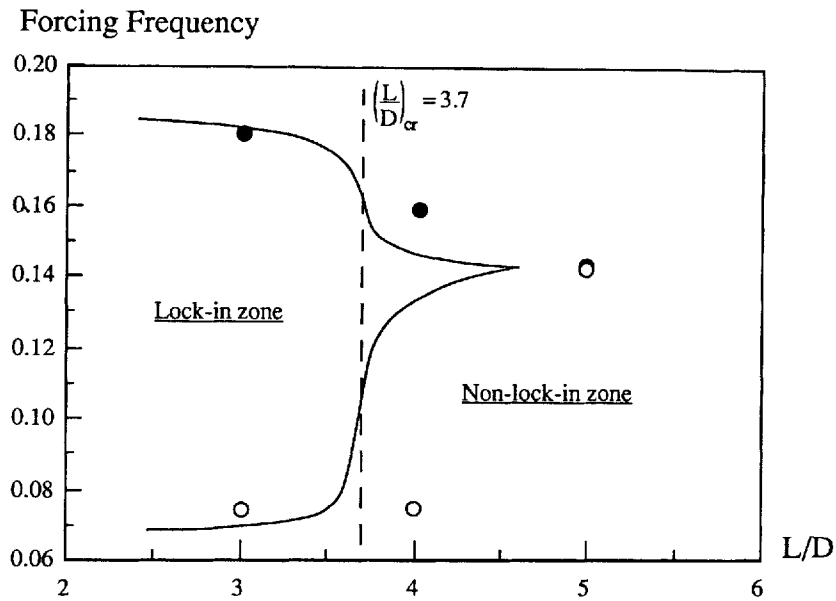

Figure 11. Lock-in region diagram ($Re=80$ and $A/2\pi f_e=0{\cdot}14$). Numerical results are represented by lines, while experimental results of Tanida *et al.*[8] are represented by circles: (○) lower limit; (●) upper limit of the lock-in zone

the forcing mechanism used in the present study has reflected the basic characteristics of wake–cylinder-oscillation–wake interactions.

5. CONCLUSIONS

The system consisting of two identical cylinders in tandem arrangement was considered in this study. Flow regimes, flow characteristics, non-linear interaction of cylinder oscillation and its upstream and downstream vortex wake are investigated. The results obtained enable us to draw the following conclusions about flow patterns and characteristics as well as about the frequency selection process of the oscillating cylinder wake:

(1) Cylinder spacing affects essentially the flow patterns around the two cylinders. At critical spacing ($(L/D)_{cr}\approx 3{\cdot}0$ for $Re=100$ and $(L/D)_{cr}\approx 3{\cdot}7$ for $Re=80$), flow changes from 'the VS regime' to 'the VF regime'. The two regimes are characterized by the changes of averaged vortex lengths, the circumferential pressure profiles of downstream cylinder as well as drag and lift coefficient variations with respect to cylinder spacings.

(2) The response state in the wake of the downstream oscillating cylinder is either periodic (lock-in state) or quasi-periodic (non-lock-in state), which is a result of non-linear interactions among its upstream, downstream wakes and its oscillation. Its lock-in zone size is directly associated with flow regimes. Increasing the cylinder spacing results in a decrease of lock-in range. In the VS regime, lock-in is much more likely to occur than it does in the VF regime.

ACKNOWLEDGEMENTS

Computations were carried out on iPSC/860 computer at Institut de Mécanique des Fluides de Marseille. We acknowledge the technical assistance of Equipe de Point d'Accès at St.-Charles.

REFERENCES

1. G. E. Karniadakis and G. S. Triantafyllow, 'Frequency selection and asymptotic states in laminar wakes', *J. Fluid Mech.*, **199,** 441 (1989).
2. C. W. van Atta and M. Gharib, 'Ordered and chaotic vortex streets behind circular cylinders at low Reynolds numbers', *J. Fluid Mech.*, **174,** 113 (1987).
3. C. H. K. Williamson, 'Oblique and parallel modes of vortex shedding in the wake of a circular cylinder at low Reynolds numbers', *J. Fluid Mech.*, **206,** 579 (1989).
4. C. Barbi, D. P. Favier, C. A. Maresca and D. P. Telionis, 'Vortex shedding and lock-on of a circular cylinder in oscillatory flow', *J. Fluid Mech.*, **170,** 572 (1986).
5. J. Li, J. Sun and B. Roux, 'Numerical study of an oscillating cylinder in uniform flow and in the wake of an upstream cylinder', *J. Fluid Mech.*, **237,** 457 (1992).
6. R. E. D. Bishop and A. Y. Hassan, 'The lift and drag forces on a circular cylinder oscillating in a flowing fluid', *Proc. Roy. Soc. Lond.*, **A227,** 51 (1964).
7. G. H. Koopmann, 'The vortex wakes of vibrating cylinders at low Reynolds numbers', *J. Fluid Mech.*, **28,** 501 (1967).
8. Y. Tanida, A. Okajima and Y. Watanabe, 'Stability of a circular cylinder oscillating in uniform flow or in a wake', *J. Fluid Mech.*, **61,** 769 (1973).
9. J. Li, A. Chambarel, M. C. Donneaud and R. Martin, 'Numerical study of laminar flow past one and two circular cylinders', *Comput. Fluids*, **19,** 155 (1991).
10. R. Chilukuri, 'Incompressible laminar flow past a transversely vibrating cylinder' *Trans. ASME, J. Fluids Eng.*, **109,** 166 (1987).
11. S. Ishigai, E. Nishikawa, K. Nishimura and K. Cho, 'Experimental study on structure of gas flow in tube banks with tube axes normal to flow. Part I. Karman vortex flow around two tubes at various spacings', *Bull. JSME*, **15** (86), 949 (1972).
12. M. M. Zdravkovich, 'Review of flow interference between two cylinders in various arrangements', *Trans. ASME, J. Fluids Eng.*, **99,** 155 (1977).